ELSEVIER

Polymer 40 (1999) 3147–3151

polymer

Cross-linking reaction of poly(4-vinylpyridine) cylindrical microdomains of poly(α-methylstyrene)-block-poly(4-vinylpyridine) films and characterization of soluble ribbon-like nanopolymers

K. Ishizu*, T. Ikemoto, A. Ichimura

Department of Polymer Science, Tokyo Institute of Technology 2-12-1, Ookayama, Meguro-ku, Tokyo 152-8552, Japan

Received 26 January 1998; revised 10 April 1998; accepted 11 June 1998

Abstract

The ribbon-like nanopolymers were prepared by the cross-linking reaction of poly(α-methylstyrene)-block-poly(4-vinylpyridine) (PMS-block-P4VP) diblock copolymer films exhibiting P4VP cylindrical microdomains with the vapour of 1,4-dibromobutane in the solid state. It was indicated from the transmission electron microscopy (TEM) and the small-angle X-ray scattering (SAXS) that these cross-linked products had a structure of ribbon-like nanopolymers. It was found from the curve fitting on the static light scattering (SLS) intensity that such nanopolymers were in agreement with the conformation of the Gaussian model.

Keywords: Ribbon-like nanopolymer; Cylindrical microdomain; Block copolymer

1. Introduction

Block and graft copolymers of incompatible block segments form microphase-separated structures in the solid state. We have established a novel synthesis method for core-shell polymer microspheres: cross-linking segregated chains in spherical microdomains of diblock copolymers [1–7]. These microspheres were stabilized even in good solvents by multiarm chains.

More recently, Eisenberg and co-workers reported that aggregates of various morphologies can be prepared from amphiphilic block copolymers in solutions of small molecule solvents [8–11]. These aggregates are made from one family of highly asymmetric polystyrene-block-poly (acrylic acid) (PS-block-PAA) or PS-block-polyethylene oxide (PEO) diblock copolymer, in which the lengths of the insoluble PS blocks are much longer than those of the soluble PAA (or PEO) blocks. These aggregates are therefore described as crew-cut. The observed morphologies include spheres, rods, vesicles, enlogated vesicles, lamellae, large compound vesicle, large compound micelles and several others. Basically, the formation of the aggregates of different morphologies depends on the copolymer composition, the initial copolymer concentration in solution and the type and concentration of added ions.

As a matter of course, these aggregates lead to deformation in a dilute solution because of the equilibrium between micelle and unimer. Therefore, the microdomain locking of block copolymer films is one of the best methods for the preparation of nanopolymers.

In this article, we carried out the cross-linking reaction of poly (α-methylstyrene)-block-poly(4-vinylpyridine) (PMS-block-P4VP) diblock copolymer films with P4VP cylindrical microdomains with the vapour of 1, 4-dibromobutane in the solid state to obtain the ribbon-like nanopolymers. The morphology and solution properties were studied in details by electron microscopy, small-angle X-ray scattering and static and dynamic light scatterings.

2. Experimental

2.1. Block copolymer synthesis and characterization

The well-defined poly (α-methylstyrene)-block-poly(4-vinylpyridine) (PMS-block-P4VP) diblock copolymer was prepared by the usual sequential anionic addition polymerization using *n*-butyl lithium as an initiator in tetrahyrofuran (THF) at $-78^{\circ}C$. The details concerning the synthesis, purification and characterization of such block copolymers

* Corresponding author. Tel.: +81-3-5735-2634; Fax: +81-3-5734-2888; E-mail: kishizu@polymer.titech.ac.jp

0032-3861/99/$ - see front matter
PII: S0032-3861(98)00476-5

were given elsewhere [12]. Table 1 lists the characteristics of the monodisperse diblock copolymer MSV1 and the microdomain spacing of a specimen cast from 1,1,2-trichloroethane (TCE).

2.2. Cross-linking of block copolymer films

The diblock copolymer film 50 μm thick was cast from 0.03 g ml^{-1} TCE solution on a Teflon sheet. The cast film was dried under vacuum for 2 days at room temperature. Cross-linking of the segregated P4VP chains in a cylinder was carried out by using quaternization with the vapour of 1,4-dibromobutane (DBB) at room temperature under the reduced pressure for 3 days. After cross-linking reaction, the films were washed with methanol and dried in high vacuum.

2.3. Morphological observations

A film specimen of diblock copolymer for the transmission electron microscopy (TEM) observations was cast from a dilute solution of TCE on a Teflon sheet for 5 days and dried under vacuum. This film was embedded in an epoxy resin and cut into ultrathin sections (about 70–100 nm thick) using an ultra microtome (Reichert–Nissei Co., Ultracut N). This specimen was exposed to the vapour of osmium tetroxide (OsO_4).

Ultrathin film specimens of ribbon-like nanopolymers were prepared by placing a drop of 0.01–1.0 wt% toluene solution on a microscope mesh coated with a carbon film and then evaporating the solvent as slowly as possible at 25°C. Morphological results were obtained on a Hitachi H-500 TEM at 75 kV.

2.4. Dilute solution properties

The weight-average molecular weight ($\bar{M}$w), the second virial coefficient (A_2), and the radius of gyration (R_G) were determined by static light scattering (SLS) in benzene at 25°C on a Photal TMLS-6000HL (Otsuka Electronic Ltd) with an He–Ne laser ($\lambda_0 = 632.8$ nm) in the Berry mode [13]. The Berry plot is often useful to apply for branched polymers. The refractive index increment dn/dc of nanopolymer was measured with a differential refractometer. The scattering angles were in the range of 30°–150°. Samples were filtered through membrane filters with nominal pores of 0.2 μm before measurement. Solutions were measured in the concentration range of 0.6–6.2 g l^{-1}.

The hydrodynamic radius (R_H) of nanopolymers was determined using a dynamic light scattering (QELS; scattering angle = 90°, Otsuka Electronics Ltd) in 0.01 wt% benzene ($\eta = 0.654$ cp, $n_D = 1.501$) solution at 25°C.

2.5. Saxs measurements

Film specimen of the nanopolymer for the small-angle X-ray scattering (SAXS) measurements was cast from a dilute solution of TCE on a Teflon sheet for 5 days and dried under vacuum. This specimen was further annealed at 120°C for 1 week under vacuum so as to have structure thermodynamically at equilibrium.

The SAXS intensity profile was measured with a rotating-anode X-ray generator (Rigaku Denki Rotaflex RTP 300RC) operated at 40 kV and 100 mA. The X-ray source was monochromatized to Cu Kα ($\lambda = 1.5418$ Å) radiation. The SAXS patterns were taken with a fine-focused X-ray source using a flat plate camera (Rigaku Denki, RU-100).

3. Results and discussion

3.1. Synthesis and morphology of ribbon-like nanopolymers

Fig. 1 shows the TEM micrograph of MSV1 diblock copolymer specimen cast from TCE. The dark portions are the selectively stained P4VP blocks. This specimen shows the texture of hexagonal P4VP cylinders in a PMS matrix. On the other hand, the thermal equilibrium morphology of MSV1 specimen (cast from toluene and annealed at 120°C) was the texture of dispersed P4VP spheres in a PMS matrix [12]. Therefore, as-cast film from TCE was taken from the metastable morphology. The absolute values of cylinder radius ($R_{c,0} = 7.9$ nm) and the nearest-neighbour distance between P4VP cylinders ($d = 22.3$ nm) are also listed in Table 1.

The segregated P4VP cylindrical domains were cross-linked using DBB vapour in the solid state. It was made clear from previous results [14–16] that the films with both P4VP spherical and lamellar shapes, which consist of continuous polystyrene segment phases, were quaternized with DBB (the degree of quaternization = 40–100 mol%) in such reaction conditions. It was also found from Volhard's titration that the cross-link densities (intermolecular and intramolecular cross-linkings) were in the range 36–42 mol%. Therefore, it can be judged that the cross-linked products prepared from cylindrical microdomains have similar values

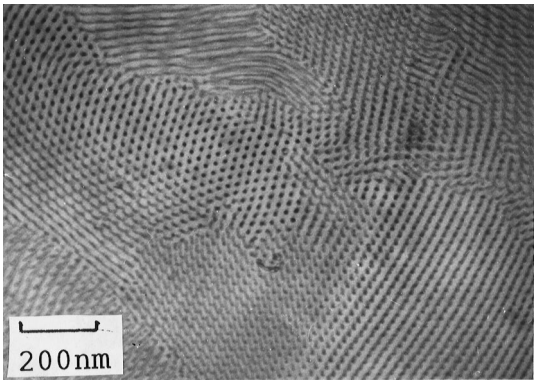

Fig. 1. TEM micrograph of diblock copolymer MSV1.

concerning the cross-link density. The cross-linked product (MSV1-N) freely dissolved in organic solvents such as benzene, toluene, THF and TCE. In order to investigate the morphology of the cross-linked products, TEM observations of the cross-linked products which had been stained with OsO_4 were carried out.

Fig. 2 shows typical TEM micrographs of MSV1-N cast from 0.01–1.0 wt% toluene solution. First, Fig. 2(a) shows TEM micrograph of MSV1-N cast from 1.0 wt% toluene solution. This specimen corresponds to the restructural film from nanopolymers. This morphology seems to be apparently PMS/P4VP alternating lamellae. Fig. 2(b) and (c) show TEM micrographs of MSV1-N cast from 0.1 and 0.01 wt% toluene solutions, respectively. In the preparation conditions of these specimens, the nanoplymers are frozen with a structure of the unimolecule on the carbon substrate. These textures show the ribbon-like morphology. Then, the morphology shown in Fig. 2(a) can be judged to the P4VP cylinders in a PMS matrix. That is to say, the cross-linked P4VP domains are not able to interpenetrate with each other and the ribbon-like nanopolymers are compatible with only the portion of PMS branches. The P4VP cylinders of MSV1 film are locked with almost the same size (P4VP cylinder radius, $R_{c,1} = 7.6$ nm) by cross-linking reactions from TEM micrographs. It is clear that these nanopolymers have only a narrow radius distribution for cross-linked P4VP cylinders. The length of the major axis (cylinder length) of the cross-linked P4VP cylinders were in the range 2040–6490 nm (average value = 3670 nm) by surveying the TEM textures.

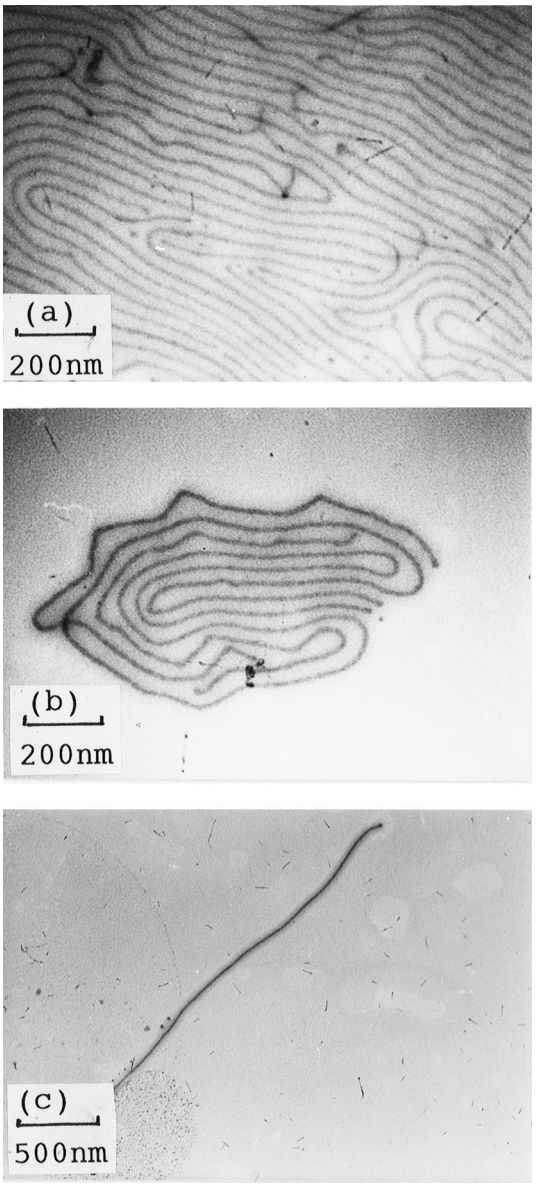

Fig. 2. TEM micrographs of nanopolymer MSV1-N, varying the concentration of toluene solutions: (a) cast from 1.0 wt%; (b) cast from 0.1 wt%; and (c) cast from 0.01 wt%.

3.2. SAXS measurements

Fig. 3 shows the SAXS intensity profile of the as-cast film of MSV1-N nanopolymer at the edge view, where $q[= (4\pi/\lambda)\sin\theta]$ is the magnitude of the scattering vector. The arrows show the scattering maxima and the values in the parentheses indicate the interplaner spacings (d_1/d_i) calculated from Bragg reflections. The first four peaks appear closely at the relative q positions of $1:\sqrt{3}:2:\sqrt{7}$ as shown by arrows. The interplaner spacing at the scattering angles is relative to the angle of the first maximum according to Bragg's equation: $2d\sin\theta = n\lambda$ (where θ is one-half the scattering angle, $\lambda = 1.5418$ Å). This packing pattern is identical to the interplaner spacing of a cylinder structure. The first interplaner spacing d_1 was estimated to be 24.2 nm from the SAXS data. It is also noticed that the observed d_1 is almost identical to the nearest-neighbour distance of cylinders ($d = 22.3$ nm: see Table 1) of the MSV1 film before the domain locking.

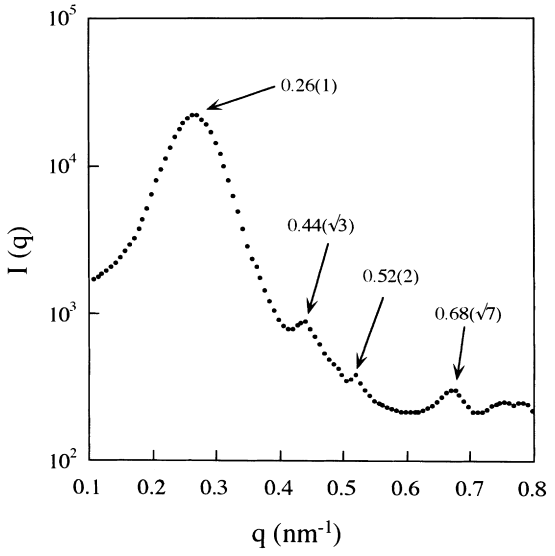

Fig. 3. SAXS intensity profile of nanopolymer MSV1-N film from edge view.

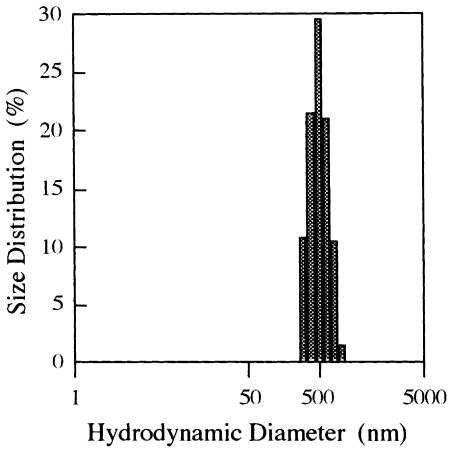

Fig. 4. Hydrodynamic diameter distribution of nanopolymer MSV1-N in benzene.

3.3. Dilute solution properties

The $\bar{M}_w$, A_2 and R_G were determined by SLS in benzene. The R_H was determined by QELS. Fig. 4 shows the hydrodynamic diameter distribution of the nanopolymer MSV1-N. The average value of R_H was determined to be 205 nm. These dilute solution properties of nanopolymer MSV1-N are listed in Table 2. It is found that this nanopolymer is composed of aggregation number $f = 3230$ of MSV1 diblock copolymers. In this work, we did not fractionate this nanopolymer by precipitation fractionation. The nanopolymers formed in the microdomains seemed to have relatively narrow molecular weight distribution because of sharp R_H distribution.

In order to obtain more information concerning the molecular conformation, we carried out the curve fitting on the SLS intensity $P(q)$ assuming to various model structures. In this work, we employed the following five models [17].

Sphere model

$$P(q) = \left[\frac{3}{X^3}(\sin X - X\cos X)\right]^2 \tag{1}$$

$X = Rq, R = \text{radius}$

Rod model, infinitely thin

$$P(q) = \frac{2}{X}\left[\int_o^x \frac{\sin t}{t}\mathrm{d}t\right] - \left(\frac{\sin X/2}{X/2}\right)^2 \tag{2}$$

$X = Lq, L = \text{rod length}$

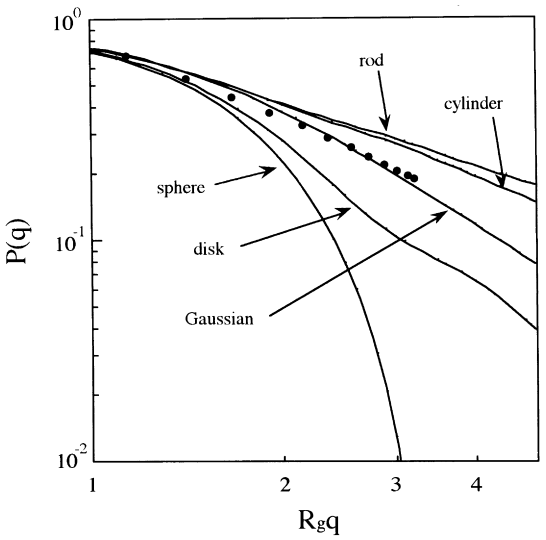

Fig. 5. Comparison between experimentally measured SLS data and theoretical calculations for five models by plotting the $P(q)$ vs $R_g q$, the closed circles indicate the observed SLS data.

Disk model, infinitely thin

$$P(q) = \frac{2}{X^2}[1 - J_1(2X)/X] \tag{3}$$

$X = Rq$, R = radius, $J_1(X)$ = Bessel function of the 1st order

Cylinder model

$$P(q) = \int_\sigma^{\pi/2} \frac{\sin^2(X_L\cos\beta)}{X_L^2\cos^2\beta} \times \frac{4J_1^2(X_R\sin\beta)}{X_R^2\sin^2\beta}\sin\beta\mathrm{d}\beta \tag{4}$$

$X_L = Lq$, $X_R = Rq$,L = cylinder length, R = radius of cylinder

Gaussian model

$$P(q) = \frac{2[\exp(-X^2) + X^2 - 1]}{X^4} \tag{5}$$

$X = q$

Fig. 5 shows the comparison between experimentally measured SLS data and theoretical calculations for five models by plotting the $P(q)$ vs Rq, where the closed circles indicate the observed SLS data. In these computer simulations, R was employed the experimental value R_G (91.4 nm). In the calculation for the cylinder model, we assumed the relation of $L/R_G = 20$. As the ratio L/R_G increases, this curve

Table 1
Characteristics of poly (α-methylstyrene)-block-poly(4-vinylpyridine) diblock copolymer and domain spacing

Specimen code	Block copolymer			Shape of P4VP domain	Domain spacing	
	$10^{-4}\overline{M}_n$ [a]	$\overline{M}_w/\overline{M}_n$ [b]	P4VP[c] block (mol%)		$R^d_{c,0}$ (nm)	d^e (nm)
MSV1	6.0	1.17	22	cylinder	7.9	22.3

[a]Determined by osmometry; [b]determined by gel permeation chromatograph; [c]determined by ^{1}H n.m.r. in $CDCl_3$; [d]radius of cylinders determined by TEM; and [e]nearest-neighbour distance between cylinders determined by TEM.

Table 2
Dilute solution properties of nanopolymer

Code	$10^{-8}\overline{M}_w$ [a]	f [b]	$10^7 A_2^a$ (mol ml g^{-2})	R_G^a (nm)	R_H^c (nm)
MSV1-N	1.93	3230	2.71	91.4	205

[a]Determined by SLS; [b]aggregation number; [c]determined by QELS.

approaches closely to that for the rod model. We find qualitative consistency between experiment and theory for the curve of the Gaussian model. On the other hand, spherical and disklike models are qualitatively inconsistent with the data. It is, thus, concluded that the nanopolymers are most probably Gaussian-like coils.

Polymerization of macromonomers provide regular multibranched polymers with a branch density. Since both the degree of polymerization and the length of branches are varied, poly(macromonomer)s are interesting models for the study of branched polymers [18–21]. Recent structure characterization of such long-chain poly(macromonomer)s revealed that the main chain exhibits an almost rodlike conformation as measured by the Kuhn statistical segment length of $1_k > 1000$ Å [22,23]. Investigations on such poly(macromonomer)s by X-ray scattering and polarized light microscopy showed the formation of lyotropic phases [24,25]. This phenomenon is based on the overcrowding of bulky side chains which forces the otherwise flexible main chains into a stretched conformation with significantly reduced degrees of freedom. The nanopolymers prepared in this work have extremely large aggregation numbers ($f = 3230$) compared to the degree of polymerizations of poly(macromonomer)s. Therefore, the main chain exhibits the Gaussian-like conformation regardless of the crowding of many branched chains.

The degree of cross-linkings (especially, intermolecular cross-linking) in the P4VP microdomains may influence strongly not only on the molecular weight but also on the molecular conformation of the nanopolymers in solution. In order to control the molecular weight and the molecular weight distribution of the nanopolymers, the most important factor may be the degree of intermolecular cross-linking. Moreover, the degree of cross-linkings may effect on the rigidity of P4VP cylinder backbone. This physical nature may be reflected on the molecular conformation of the nanopolymers in solution such as Gaussian and rod, etc. So, it is necessary to study the cross-linking reaction of P4VP microdomains in details. We are also investigating to apply for functional nanomaterials. The results obtained will be reported in the near future.

References

[1] Ishisu K, Fukutomi T. J Polym Sci, Polym Lett Ed 1988;26:281.
[2] Ishizu K. Polymer 1989;30:793.
[3] Ishizu K. Polym Commun 1989;30:209.
[4] Ishizu K, Onen A. J Polym Sci, Polym Chem Ed 1989;27:3721.
[5] Saito R, Kotsubo H, Ishizu K. Eur Polym J 1991;27:1153.
[6] Saito R, Kotsubo H, Ishizu K. Polymer 1992;33:1073.
[7] Ishizu K, Saito R. Polym-Plast Technol Engng 1992;31:607.
[8] Zhang L, Eisenberg A. Science 1995;268:1728.
[9] Zhang L, Eisenberg A. J Am Chem Soc 1996;118:3168.
[10] Yu K, Eisenberg A. Macromolecules 1996;29:6359.
[11] Zhang L, Eisenberg A. Macromol Symp 1997;113:221.
[12] Ishizu K, Ikemoto T, Ichimura A. Polymer 1998;39:449.
[13] Katime I, Quintana JR. In: Booth C, Price C, editors. Comprehensive polymer science, vol. 1, chap. 3. Oxford: Pergamon Press, 1989.
[14] Ishizu K, Inagaki K, Fukutomi T. J Polym Sci, Polym Chem Ed 1985;23:1099.
[15] Ishizu K. Polymer 1989;30:793.
[16] Saito R, Kotsubo H, Ishizu K. Polymer 1994;35:1747.
[17] Burchard W. Adv Polym Sci 1983;48:1.
[18] Tsukahara Y, Tsutsumi K, Okamoto Y. Macromol Rapid Commun 1992;13:409.
[19] Tsukahara Y, Mizuno K, Segawa A, Yamashita Y. Macromolecules 1989;22:1546.
[20] Tsukahara Y, Tsutsumi K, Yamashita Y, Shimada S. Macromolecules 1989;22:2869.
[21] Tsukahara Y, Tsutsumi K, Yamashita Y, Shimada S. Macromolecules 1990;23:5201.
[22] Wintermantel M, Schmidt M, Tsukahara Y, Kajiwara K, Kohjiya S. Macromol Rapid Commun 1994;15:279.
[23] Wintermantel M, Gerie M, Fischer K, Schmidt M, Wataoka I, Urakawa H, Kajiwara K, Tsukahara Y. Macromolecules 1996;29:978.
[24] Tsukahara Y, Ohta Y, Senoo K. Polymer 1995;36:3413.
[25] Wintermantel M, Fischer K, Gerie M, Ries R, Schmidt M, Kajiwara K, Urakawa H, Wataoka I. Angew Chem Int Ed Engl 1995;34:1472.